

---

# Continual Learning of Multi-modal Dynamics with External Memory

---

**Abdullah Akgül**

Istanbul Technical University  
Istanbul, Turkey  
akgula15@itu.edu.tr

**Gozde Unal**

Istanbul Technical University  
Istanbul, Turkey  
gozde.unal@itu.edu.tr

**Melih Kandemir**

University of Southern Denmark  
Odense, Denmark  
kandemir@imada.sdu.dk

## Abstract

We study the problem of fitting a model to a dynamical environment when new modes of behavior emerge sequentially. The learning model is aware when a new mode appears, but it does not have access to the true modes of individual training sequences. We devise a novel continual learning method that maintains a descriptor of the mode of an encountered sequence in a neural episodic memory. We employ a Dirichlet Process prior on the attention weights of the memory to foster efficient storage of the mode descriptors. Our method performs continual learning by transferring knowledge across tasks by retrieving the descriptors of similar modes of past tasks to the mode of a current sequence and feeding this descriptor into its transition kernel as control input. We observe the continual learning performance of our method to compare favorably to the mainstream parameter transfer approach.

## 1 Introduction

*Continual Learning (CL)* aims to develop a versatile model that is capable of solving multiple prediction tasks which are presented to the model one task at a time. The model is then expected to learn the latest task as accurately as possible while preserving its excellence at the previous ones. Performance drop caused by the newly learned task is called *catastrophic forgetting*. Continual learning is essential for the development of intelligent agents that can adapt to new environmental conditions not encountered during training. For instance, an autonomous driving controller may improve its policy based on new experience collected during its customer-side life time. There exist a solid body of work that adopt parameter transfer across tasks as the key element of task memorization [23, 26, 32, 38]. There also appear preliminary studies on building attentive memories to capture tasks [11, 9]. Principles that yield memory mechanisms optimal for continual learning are yet to be discovered.

Probabilistic State-Space Models (SSM) are the standard framework for uncertainty-aware identification of complex dynamical systems. SSMs find widespread applicability to forecasting socio-economically impactful quantities such as weather, currency exchange, equity prices, and sales trends. SSM research gains significance also in robot learning parallel to the growing interest in model-based reinforcement learning [4, 16, 15]. SSMs also set the fundamentals of stochastic optimal control [1], enhancing the impact potential of their thorough investigation even further.

We introduce a novel problem setup where dynamical system modeling tasks emerge sequentially and a probabilistic SSM is expected to learn them cumulatively. We further assume each task to follow multi-modal dynamics, where each individual sequence of a task follows one of the possible modes that describe the task. Successful continual learning in such a setup presupposes maximally efficient encoding of tasks into a long-term memory and their accurate retrieval. We curate a novel continual learning model tailored for addressing this challenging problem. Our model captures the characteristics of unknown modes of sequences of the present task into fixed-sized vectors, called

*mode descriptors*, stores these descriptors in an external neural episodic memory addressable via a learnable attention mechanism. Our model represents multiple task modes by feeding these mode descriptors into the state transition kernel as an additional input. We place a Dirichlet Process prior on the attention weights of the memory to encourage the explanation of the data with minimum number of modes. Figure 1 illustrates our model with external memory and the problem with two tasks and four modes. Our resulting Bayesian model can be efficiently trained using a straightforward adaptation of existing variational SSM inference techniques.

We evaluate our model in two real-world time series prediction data sets and three synthetic data sets generated from three challenging nonlinear multi-modal dynamical systems. Our method exhibits consistent performance improvement over the established parameter transfer approach, verifying the importance of parsimonious use of neural episodic memory in efficient within-task knowledge acquisition and effective cross-tasks knowledge transfer.

## 2 Problem Setup: Continual Multi-Modal Dynamics Learning

We assume a learning agent that observes a dynamical environment via sequences  $y_{1:T} = \{y_1, \dots, y_T\}$  consisting of time-indexed measurements  $y_t \in \mathcal{Y}$  living in a measurable space  $\mathcal{Y}$ . We denote a snippet of a sequence  $y_{t:t'} = \{y_t, \dots, y_{t'}\}$  for an arbitrary time interval  $[t, t']$ . Modes refer to general distinguishable properties of a dynamic system such as states with different characteristics of sine wave (amplitude, frequency) or semantically different dynamics such as different character trajectories. We refer all these factors as modes. We define the *mode* of a sequence  $y_{1:T}$  as a fixed-sized vector and  $m$  as an element of a  $K$ -dimensional embedding space  $\mathcal{X}$ . A dynamical system can potentially operate within a large number of modes. Making an analogy to the real world, an autonomous vehicle accounts for different environmental characteristics when planning and control for different weather conditions, countries, and times of a day. Only few of the modes are active for a particular time point and each mode instantly activates and deactivates for limited time periods.

We search for a learning algorithm that enables the agent to fit to a dynamical environment which has perpetually changing global characteristics. *We cast the corresponding learning problem as continual learning of multi-modal dynamical systems, where each task is defined as a group of modes that modulate a specific dynamical system.* In formal terms, a task  $\mathcal{T}_i$  is defined as a group of mode descriptors sampled from a mode generating oracle  $P(\mathcal{X})$ , that is

$$\mathcal{T}_i = \{m_r | m_r \sim P(\mathcal{X}), r = 1, \dots, R\}, \quad i = 1, \dots, U, \quad (1)$$

where  $R$  is number of modes and  $U$  is number of tasks. We assume that each sequence of a task follows dynamics modulated by a mode sampled from  $\mathcal{T}_i$

$$\mathcal{D}_{\mathcal{T}_i} = \left\{ y_{1:T}^n \mid m_n \sim P(\mathcal{T}_i), y_{1:T}^n \sim p(y_{1:T} | m_n), n = 1, \dots, N \right\}, \quad (2)$$

where  $P(\mathcal{T}_i)$  is a probability mass function defined on the modes of task  $\mathcal{T}_i$  and  $p(y_{1:T} | m_r)$  is the probability measure that describes the true behavior of the environment dynamics under mode  $m_r$  within a time interval  $[1, T]$ . The marginal distribution of a task with respect to its modes is given as

$$p(y_{1:T} | \mathcal{T}_i) = \sum_{r=1}^R p(y_{1:T} | m_r) P(m_r | \mathcal{T}_i). \quad (3)$$

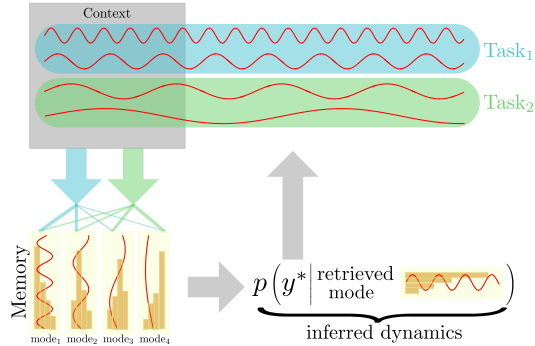


Figure 1: We study continual learning of dynamical systems, each operate on a non-overlapping set of multiple modes unknown to the learner at each task. We find out that inferring mode descriptors from an observed sequence snippet ( $y_{1:C}$ ), storing them in an external neural episodic memory, retrieving them in the subsequent tasks, and feeding them into the state transition kernel as control input brings improved continual learning performance. We encourage efficient use of memory space by placing a Dirichlet Process (DP) prior on the effective count of encountered modes.

The agent observes a task via a data set  $\mathcal{D}_{\mathcal{T}_i}$  that contains only the sequences  $y_{1:T}^n$  *but not their corresponding modes*.

We are interested in learning a model that minimizes the true continual learning risk functional below

$$R_{\mathbb{L}}^{CL}(h_{\theta}) = \lim_{U \rightarrow +\infty} \sum_{i=1}^U \mathbb{E}_{\mathcal{T}_i \sim P(\mathcal{X})} \left[ \mathbb{E}_{y_{1:T} \sim p(y_{1:T} | \mathcal{T}_i)} \left[ \mathbb{L}(h_{\theta}(\cdot | y_{1:C}), y_{C+1:T}) \right] \right], \quad (4)$$

which amounts to the limit of the cumulative risk of individual tasks as they appear one at a time. Above,  $h_{\theta} : \mathcal{Y}^C \rightarrow \mathcal{Y}^{T-C}$  is a stochastic process that can map an observed sequence of an arbitrary length  $C$  to the subsequent  $T - C$  time steps. We call the first  $C$  observations in the sequence  $y_{1:C}$  as the *context* and define  $\mathbb{L}$  as a sequence-specific loss function defined on the future values of the sequence  $y_{C+1:T}$ . We evaluate the performance of predictions  $\hat{y}$  via two scores:

**Normalized Mean Squared Error (NMSE):**

$$\mathbb{L}_{NMSE}(h_{\theta}(\cdot | y_{1:C}), y_{C+1:T}) = \mathbb{E}_{\hat{y}_{C+1:T} \sim h_{\theta}(\cdot | y_{1:C})} \left[ \frac{\|\hat{y}_{C+1:T} - y_{C+1:T}\|_2^2}{\|y_{C+1:T}\|_2^2} \right] \quad (5)$$

as a measure of the prediction accuracy of  $h_{\theta}$  when used as a Gibbs predictor, and

**Negative Log-likelihood (NLL):**

$$\mathbb{L}_{NLL}(h_{\theta}(\cdot | y_{1:C}), y_{C+1:T}) = \log h_{\theta}(\hat{y}_{C+1:T} | y_{C+1:T}) \quad (6)$$

as a measure of Bayesian model fit that quantifies the model’s own assessment on the uncertainty of its assumptions.

We approximate the true continual learning risk by its empirical counterpart

$$\hat{\mathbb{R}}_{\mathbb{L}}^{CL} = \frac{1}{N} \sum_{i=1}^U \sum_{n=1}^N \mathbb{L}(h_{\theta}(y_{C+1:T}^n | y_{1:C}^n) | \mathcal{T}_i) \quad (7)$$

for a finite number  $U$  of tasks presented to  $h_{\theta}$  one at a time.

### 3 Novel Baseline: Variational Continual Learning for Bayesian State-Space Models

We build our target model on a Bayesian treatment of state-space modeling, which is proven to be effective in learning under high uncertainty and knowledge transfer across tasks, as practiced in the seminal prior art of continual learning [23, 26]. We perform approximate inference using variational Bayes due to its multiple successful applications to state-space models [10, 5, 19] and its favorable computational properties. *As there does not exist any prior work tailored specifically towards continual learning for dynamical systems, we curate our own baseline.* We adopt the established practice of setting the posterior of the learned parameters of the previous task as the prior of the next one and determine Variational Continual Learning (VCL) [26] as the state-of-the-art representative of this approach. Elastic Weight Consolidation (EWC) [23] also follows the same approach but uses a simpler posterior inference scheme.

**Bayesian State Space Models (BSSM)** are characterized by the data generating process below

$$\begin{aligned} \theta &\sim p(\theta), & x_0 &\sim p(x_0), \\ x_t | x_{t-1}, \theta &\sim p(x_t | x_{t-1}, \theta), & y_t | x_t &\sim p(y_t | x_t), \end{aligned} \quad (8)$$

where  $x_t$  and  $y_t$  correspond to the latent and observed state variables for time step  $t$ , respectively. The system dynamics are modeled by the first-order Markovian transition kernel  $p(x_t | x_{t-1}, \theta)$  parameterized by  $\theta$  that in turn follows a prior distribution  $p(\theta)$ . The latent states are mapped to the observation space via a probabilistic observation model  $p(y_t | x_t)$ . We formulate the initial latent state  $x_0$  as another random variable that follows the prior distribution  $p(x_0)$ .

**Variational Inference** is required to approximate the posterior  $p(x_{0:T}, \theta | y_{1:T})$ , which will be intractable for many choices of distribution families for the data generating process in Eq. 8. Following [37], we choose the variational distribution to be mean-field across the parameters of the dynamics and the latent states  $q_{\xi, \psi}(x_{0:T}, \theta | y_{1:T}) = q_{\xi}(x_0 | y_{1:C}) \prod_{t=1}^T p(x_t | x_{t-1}, \theta) q_{\psi}(\theta)$ , where  $q_{\xi, \psi}$  is an approximation to the true posterior  $p(x_{0:T}, \theta | y_{1:T})$  with variational free parameters  $(\xi, \psi)$ . This formulation has multiple advantages. Firstly, modeling the marginal posterior on the initial latent state  $x_0$  by amortizing on the context observations  $y_{1:C}$  makes the Evidence Lower Bound (ELBO) calculation invariant to the context length. Secondly, adopting the prior transition kernel avoids duplicate learning of environment dynamics with twice as many free parameters and prevents training from instabilities caused by the inconsistencies between prior and posterior dynamics. We provide corresponding ELBO and its derivation in Appendix A.1.1.

**VCL for BSSMs** can be implemented as follows. Having fitted the ELBO (Eq. 17) ( $\mathcal{L}$ ) on the data set for the first task which has observed sequences  $\mathcal{D}_{\mathcal{T}_1}$ , we attain  $(\xi_1^*, \psi_1^*) = \operatorname{argmax}_{\xi, \psi} \mathcal{L}(\xi, \psi, \mathcal{D}_{\mathcal{T}_1})$ . When the next task arrives with data  $\mathcal{D}_{\mathcal{T}_2}$ , we assign  $p(\theta) \leftarrow q_{\psi_1^*}(\theta)$  and maximize the ELBO again  $(\xi_2^*, \psi_2^*) = \operatorname{argmax}_{\xi, \psi} \mathcal{L}(\xi, \psi, \mathcal{D}_{\mathcal{T}_2})$ . We repeat this process continually for every new coming task. We refer to this newly curated baseline in the rest of the paper as *VCL-BSSM*. We neglect the coresets extension of VCL since its application to BSSMs is tedious and its advantage is not demonstrated with sufficient significance in the static prediction tasks studied in the original work.

## 4 Target Model: The Continual Dynamic Dirichlet Process

The commonplace Bayesian approach to continual learning transfers knowledge across tasks by assigning the learned posterior on the parameters of the previous task as the prior on the parameters of the current task. This is an effective approach when the subject of transfer is a feed-forward model, such as a classifier in supervised learning setup [26] or a policy network in reinforcement learning [23]. *We conjecture that the existing parameter transfer Ansatz would not be sufficient for the transfer of more complex task properties such as modes of dynamical systems.* We address this problem by tailoring a novel continual learning approach from an original combination of an aged statistical machine learning tool, the Dirichlet process, with modern neural episodic memory and attention mechanisms.

**Dirichlet Processes** are stochastic processes defined on a countably infinite number of categorical outcomes, every finite subset of which follows a multinomial distribution drawn from a Dirichlet prior [35]. A Dirichlet Process (DP) follows a Griffiths-Engen-McCloskey (GEM) distribution [27]

$$\pi'_r | \alpha_0 \sim \text{Beta}(1, \alpha_0), \quad \pi_r = \pi'_r \prod_{j=1}^{r-1} (1 - \pi'_j), \quad \pi = [\pi_1, \dots, \pi_R], \quad (9)$$

which we denote in short hand as  $\pi \sim \text{GEM}(\alpha_0, R)$ . The GEM distribution can also be viewed as a stick-breaking process [31, 8] where  $\alpha_0 > 0$  is a scalar hyper-parameter. The data generation process below is called a Dirichlet Process for a base measure  $G_0(\mathcal{X})$  defined on a  $\sigma$ -algebra  $\mathbb{B}$  of  $\mathcal{X}$

$$m_r \sim G_0(\mathcal{X}), \quad \pi \sim \text{GEM}(\alpha_0, R), \quad G | \pi = \sum_{r=1}^R \pi_r \delta_{m_r}, \quad (10)$$

where  $\delta_x(A)$  is Dirac delta measure that takes value 1 if  $x \in A$  and 0 otherwise for any measurable set  $A \in \mathbb{B}$  and  $G$  is a categorical distribution with parameters  $\pi$ .

**Neural Episodic Memory.** We assume that the environment dynamics can be expressed within a measurable latent embedding space  $x_t \in \mathcal{X}$ , and a sequence encoder  $e_{\lambda}(x_{t:t'})$  parameterized by  $\lambda$  for  $t \leq t'$  that maps a sequence of latent embeddings into a fixed dimensional vector, as well as a neural memory  $M = \{m_1, \dots, m_R\}$  consisting of  $R$  elements  $m_r \in \mathcal{X}$  that live in the same space as latent embeddings  $x_t$ . We can construct a probability measure for  $\mathbb{B}$  from the memory  $M$  by updating

$$m_r \leftarrow (1 - w_r(y_{1:C}, m_r))m_r + w_r(y_{1:C}, m_r)e_{\lambda}(y_{1:C}) \quad (11)$$

for each sequence where  $w_r(y_{1:C}, m_r) = e^{\langle m_r, e_{\lambda}(y_{1:C}) \rangle} / \sum_{j=1}^R e^{\langle m_j, e_{\lambda}(y_{1:C}) \rangle}$  for some similarity function  $\langle \cdot, \cdot \rangle : \mathcal{X} \times \mathcal{X} \rightarrow \mathbb{R}^+$ . This construction imposes a memory attention mechanism, where the

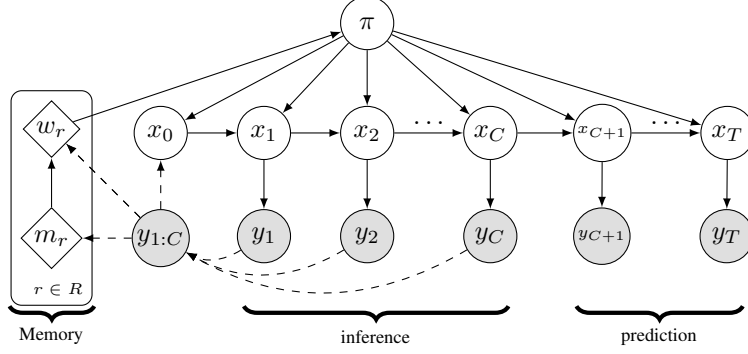


Figure 2: *CDDP Plate Diagram*. Shaded nodes are observed, unshaded nodes are latent and diamonds are deterministic. Solid arrows denote the conditional dependencies of the true model and dashed arrows denote the same for the approximate posterior. The first  $C$  observations, called *the context*, amortize the inference of the initial hidden state, and also determine the content and addressing of the mode embeddings in the external memory.

encoded mode descriptors attend to the memory elements. Here we make the fair assumption that the modality of a sequence can be identified also from the observation space, while we need to infer the latent representations accurately to model the mode dynamics in detail. We choose an uninformative base measure that assigns equal prior probabilities to memory elements  $G_0(M) = \sum_{k=1}^R \frac{1}{R} \delta_{m_r}$ .

**The full model.** We complement the BSSM in Eq. 8 with an external neural episodic memory  $M$  that is updated for each observed sequence with the rule in Eq. 11. We place a DP prior on the retrieval of mode descriptors  $m_r \in M$  to encourage the model to generate a minimum number of modes. We also feed the retrieved mode descriptor into the transition kernel  $p(x_t|x_{t-1}, m, \theta)$  as control input. The resultant model, which we call as the *Continual Dynamic Dirichlet Process (CDDP)*, follows the generative process

$$\begin{aligned} \pi &\sim GEM(\alpha_0, R), & m|\pi &\sim \sum_{r=1}^R \pi_r \delta_{m_r}, & \theta &\sim p(\theta), \\ x_0 &\sim p(x_0), & x_t|x_{t-1}, m, \theta &\sim p(x_t|x_{t-1}, m, \theta), & y_t|x_t &\sim p(y_t|x_t), \end{aligned} \quad (12)$$

where the memory capacity  $R$  is set to a bigger number than the expected upper limit of the mode count. Figure 2 summarizes the CDDP model design.

**Inference.** Since  $p(x_{0:T}, \theta|y_{1:T})$  is intractable, we approximate it by variational inference. We inherit the advantages of the BSSM inference scheme by choosing the variational distribution as

$$q_{\xi, \psi}(x_{0:T}, \theta, \pi|y_{1:T}) = q_{\xi}(x_0|y_{1:C}, \pi) \prod_{t=1}^T \sum_{r=1}^R q_{\xi}(\pi = r|y_{1:C}) p(x_t|x_{t-1}, m_r, \theta) q_{\psi}(\theta), \quad (13)$$

where

$$\begin{aligned} q_{\psi}(\theta) &= \mathcal{N}(\theta|\mu, \Sigma), & q_{\xi}(\pi|y_{1:C}) &= Cat(w_1(m_1, y_{1:C}), \dots, w_K(m_R, y_{1:C})), \\ q_{\xi}(x_0|y_{1:C}, \pi) &= \sum_{r=1}^R \pi_r \mathcal{N}\left(x_0 \middle| v_1(m_r, e_{\lambda}(y_{1:C})), v_2(m_r, e_{\lambda}(y_{1:C}))\right) \end{aligned} \quad (14)$$

with  $x_0 \sim \mathcal{N}(0, I)$ . In the expressions above,  $v_1$  and  $v_2$  refer to dense layers. The corresponding ELBO is then calculated following similar lines to Eq. 17 (see Appendix A.1.2 for derivation)

$$\begin{aligned} \log p(y_{1:T}) &\geq \sum_{r=1}^R q_{\xi}(\pi = r|y_{1:C}) \mathbb{E}_{p(x_{1:T}|\theta, x_0, m_r) q_{\xi}(x_0|y_{1:C}) q_{\psi}(\theta)} [\log p(y_{1:T}|x_{1:T})] \\ &\quad - KL(q_{\xi}(x_0|y_{1:C})||p(x_0)) - KL(q_{\psi}(\theta)||p(\theta)) - \sum_{r=1}^R w_r(m_r, y_{1:C}) \log(w_r(m_r, y_{1:C})/\pi_r), \end{aligned} \quad (15)$$

where  $KL(\cdot||\cdot)$  stands for Kullback-Leibler (KL) divergence.

**Prediction.** Having trained the model on the latest task  $\mathcal{T}_i$ , its posterior predictive distribution for a new sequence  $Y^*$  and corresponding latent embeddings  $X = \{x_0, \dots, x_T\}$  can be computed as

$$p(Y_{C+1:T}^* | \mathcal{D}_{\mathcal{T}_i}, Y_{1:C}^*) = \sum_{r=1}^R q(\pi = r | Y_{1:C}^*) \int_{X, \theta} q_{\xi}(x_0 | Y_{1:C}^*, \pi = r) q_{\psi}(\theta) \left[ \prod_{t=C+1}^T p(y_t^* | x_t) p(x_t | x_{t-1}, \theta, m_r) \right]. \quad (16)$$

## 5 Related Work

**State Space Models.** Deterministic SSMs, such as the Long Short-Term Memory (LSTM) [18], the Gated Recurrent Unit (GRU) [3], and Transformer Nets [36] are in frequent use for sequential predictions. There exist a considerable body of work on Bayesian versions of SSMs that employ Gaussian Process as transition kernels [10, 5, 19] and perform variational inference. Another vein of work named Recurrent State-Space Models (RSSMs) [9, 16, 15] models the transition dynamics as Recurrent Neural Nets (RNN) that map a state to the next time step deterministically, while admitting a random state variable from the previous time step as input and feeding its output to the distribution of this variable at the subsequent time step.

**Attention and Memory in Neural Nets.** Neural Turing Machines (NTMs) [12] and Differential Neural Computers (DNC) [13] are first examples of attention-based neural episodic memory use with external updates. Transformer Networks [36] introduce the notion of self attention and effectively use it in conjunction with cross attention to perform sequence-to-sequence prediction for long horizons. The Attentive Neural Process (ANP) [21] employs attention network to build a neural stochastic process that is consistent over the observed predictions. It has been shown that an attention network can also be viewed as a Hopfield Network [28], which explains its success at memorization of complex patterns. The Evidential Turing Process (ETP) [20] maintains an external memory that learns to feed a Dirichlet prior on the class distribution with informative concentration parameters inferred during minibatch training updates.

**Continual Learning** is an instance of meta learning [7, 33] where new tasks are introduced one at a time and a base model is expected to learn the newest task without forgetting the previous ones. Unlike biological intelligence, artificial intelligence suffers from catastrophic forgetting in continual/lifelong learning. Early approaches to continual learning such as Synaptic Intelligence (SI) [38] and Elastic Weight Consolidation (EWC) [23] transfer knowledge by the transfer of either deterministic parameters or their inferred distribution. SI calculates a plasticity measure by comparing the change rate of the gradients of the loss and the change rate of the synapses, whereas EWC uses Fisher information. Variational Continual Learning (VCL) [26] improves on EWC with a more comprehensive inference scheme and an additional feedback channel via a core set of most characteristic observations of past tasks. Generalized VCL (GVCL) [24] maximizes the same ELBO as VCL but using  $\beta$ -VAE to prevent the training instability caused by the dominance of the KL-divergence term. We do not use  $\beta$ -VAE since our setup does not have this problem. Sequential Neural Processes (SNP) [32] captures the evolution of parameters across tasks via a recurrent SSM that determines the sufficient statistics of a neural process prior. For the first time, our CDDP studies multi-modality in a continual learning setting. It is also the first model to transfer knowledge across tasks via learned mode descriptors that are maintained in an external memory.

**Continual Learning with Episodic Memory.** Closed-loop memory replay GAN (CloGAN) [29] builds a memory by maximum sample diversity in order to reduce catastrophic forgetting by remembering samples of previous tasks. Generative Memory Net (GMNet) [34] creates a memory with two GANs in order to generate adversarial samples for previous tasks to be used in the new task. In [14], a memory keeps sample random examples from previous tasks and these samples are used in the training of the new tasks. There are other works [25, 2] that uses memory for continual learning however, all of them build the memory with the help of data points provided with the ground truth but in our setup mode labels are not provided. Hence our work is not comparable to theirs. As neither of them studies dynamics modeling, their adaption to our setup is not straightforward.

## 6 Experiments

We evaluate the performance of CDDP rigorously on five challenging applications of continual learning to time series forecasting.

**Baseline Selection.** As we are the first to investigate continual learning for BSSM inference, there is no prior work we can take as a baseline without significant adaptation. We determine knowledge transfer across tasks by setting the parameter posterior of the previous task as the prior of the next as the state of the art approach in continual learning. We adapt VCL, the most established variant of this approach, to BSSMs in Section 3 as a baseline that can maximally challenge our CDDP.

**Hyper-parameter Selection.** Unlike many commonplace continual learning benchmark setups that do few-way low-dimensional image classification, BSSM inference of even a single dynamical system necessitates careful tuning of hyper-parameters. Thus, we set latent state dimensionality, learning rate, and the hidden layer sizes of the encoder, transition kernel, and decoder networks to values that maximize the performance of the BSSM on the first task. Notably, the selection favors VCL and CDDP equally. See Appendix A.2 for further details on the chosen hyper-parameter values.

### 6.1 Synthetic Data Sets

We evaluate our CDDP on three nonlinear dynamical systems, where forecasting is challenging, while ground-truth task similarity is controllable. Too much task similarity would make continual learning unnecessary, while too much task difference would make it infeasible. When tasks share a reasonable degree of similarity, a successful continual learning algorithm is expected to capture, encode, and memorize these similarities and discard their differences. We perturb all three dynamical systems with Gaussian white noise.

We generate modes that share similar dynamical properties, as their time evolution follows the same set of differential equations. However, modes differ from each other in the choice of

the free parameters that govern the dynamical system. **i) Sine Waves** data set consists of signals grouped into modes described by different magnitudes and frequencies. Sine waves are created from the function  $A\sin(2\pi ft)$  where  $A$  is the magnitude,  $f$  is the frequency, and  $t$  is time. We generate different modes from five different choices for magnitudes and three frequency levels. **ii) Lotka-Volterra** equations stem from modeling the dynamics of predator and prey populations and are defined as the nonlinear differential equations:  $dx_t/dt = \alpha x_t - \beta x_t y_t$ ,  $dy_t/dt = \delta x_t y_t - \gamma y_t$ . We generate different modes by setting the free parameter pairs  $(\alpha, \delta)$  and  $(\beta, \gamma)$  to different values. **iii) Lorenz Attractor** is a three-dimensional nonlinear dynamical system developed originally to model atmospheric convection. As the Lorenz attractor is chaos-theoretic, hence not solvable with predictable consistency using the existing numerical methods, it is often used as a challenging environment to evaluate probabilistic dynamical models [17, 30]. The Lorenz system is described by  $dx_t/dt = \sigma(y_t - x_t)$ ,  $dy_t/dt = x_t(\rho - z_t) - y_t$ ,  $dz_t/dt = x_t y_t - \beta z_t$ . We determine our modes by settings the free parameters  $\sigma, \rho$ , and  $\beta$  of the Lorenz system to different values. Figure 3 presents a sample visualization of modes that constitute the continual learning tasks on each of the three dynamical systems. We provide choice of the free parameters that differ the modes in Appendix A.2.

### 6.2 Real-World Data Sets

We evaluate our CDDP in two real-world data sets from [6]. **i) Libras Movement Data Set** is the official Brazilian sign language and acronym of the Portuguese name "Língua BRAsileira de Sinais". The data set consists of sequences of  $(x, y)$  coordinates of hand movements from 15 different classes. **ii) Character Trajectories** data set consists of sequences of velocities of  $(x, y)$  coordinates and pen

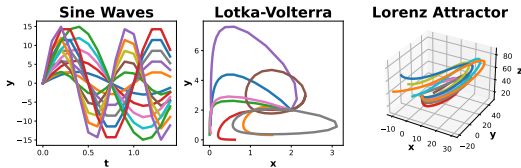


Figure 3: Sample sequences collected from different modes of the dynamical systems from synthetic data sets. Colors correspond to different modes. For each data set, modes live in the same dynamical system but differ in the free parameters that govern the dynamics. For instance, the Sine Waves differ in magnitude and frequency.

Table 1: The summary of our main results given as the Area Under Curve (AUC) plotting the change of two performance metrics *Normalized Mean Squared Error (NMSE)* and *Negative Log-Likelihood* as a function of the number of learned tasks. The reported numbers are mean  $\pm$  standard error over 10 repetitions. The detailed results are provided in Table 3. Our CDDP outperforms VCL-BSSM in nearly all cases indicating the benefit of maintaining an external memory of mode descriptors in continual learning, the central hypothesis of this work.

Data Set	AUC NMSE		AUC NLL	
	VCL-BSSM	CDDP	VCL-BSSM	CDDP
Sine Waves	1.00 $\pm$ 0.04	<b>0.91 <math>\pm</math> 0.03</b>	3.57 $\pm$ 0.09	<b>3.50 <math>\pm</math> 0.09</b>
Lotka-Volterra	<b>0.58 <math>\pm</math> 0.04</b>	0.60 $\pm$ 0.06	1.50 $\pm$ 0.05	<b>1.32 <math>\pm</math> 0.08</b>
Lorenz Attractor	0.26 $\pm$ 0.00	<b>0.24 <math>\pm</math> 0.01</b>	4.42 $\pm$ 0.04	<b>4.35 <math>\pm</math> 0.06</b>
Libras	<b>0.14 <math>\pm</math> 0.00</b>	<b>0.14 <math>\pm</math> 0.00</b>	-0.37 $\pm$ 0.02	<b>-0.39 <math>\pm</math> 0.04</b>
Character Trajectories	0.87 $\pm$ 0.04	<b>0.64 <math>\pm</math> 0.01</b>	0.14 $\pm$ 0.02	<b>-0.19 <math>\pm</math> 0.03</b>

force collected from hand-writings of 20 English alphabet characters, which can be written by a single pen-down segment. Treating each class as a mode, we generate multimodal time series forecasting tasks from these two data sets that satisfy the learning setup in Eq. 4.

### 6.3 Results and Ablation Study

**Main Results.** Table 1 summarizes model performance throughout the whole continual learning process as the area under learning curve. Our CDDP outperforms the parameter transfer based VCL-BSSM baseline consistently in nearly all cases. Storing mode descriptors of the learned dynamics in an external memory, retrieving them in the subsequent tasks, and feeding them into the state transition kernel prevents catastrophic forgetting more effectively than plain parameter transfer. As seen in Figure 4, in the challenging character trajectories dataset, the prediction accuracy of our CDDP significantly outperforms VCL-BSSM in both early and late stages of the continual learning period.

**Computational Cost.** The difference of the computational footprints of our neural episodic memory based approach and the parameter transfer approach is negligible. The average wall-clock Time Per Epoch (TPE) measured on the Sine Wave data set is  $0.20 \pm 0.00$  seconds for VCL-BSSM and  $0.21 \pm 0.00$  seconds for CDDP. The computational cost of CDDP increases linearly with memory size, which is balanced by its parsimonious memory usage by virtue of the Dirichlet Process prior.

**Ablation Study.** We investigate the contribution of individual design choices to the total performance of our target model. We study the effect of three design choices: i) knowledge transfer via parameters  $\theta$  of the learned transition dynamics, ii) quantifying the uncertainty of the parameters of transition dynamics by a distribution  $q_\psi(\theta)$ , and iii)

Table 2: Ablation study results given as the Area Under Curve (AUC) on the Sine Waves data set. The reported numbers are mean  $\pm$  standard error over 5 repetitions.

	Parameter Transfer	Probabilistic Parameters	Memory Content	NMSE	NLL
RNN	✓	×	N/A	1.03 $\pm$ 0.05	3.50 $\pm$ 0.10
VCL-BSSM	✓	✓	N/A	0.93 $\pm$ 0.03	3.59 $\pm$ 0.16
CDDP Variants	×	✓	Zeros	0.94 $\pm$ 0.04	3.56 $\pm$ 0.12
	×	✓	Ones	1.12 $\pm$ 0.13	3.75 $\pm$ 0.14
	✓	✓	Twos	1.35 $\pm$ 0.23	3.80 $\pm$ 0.18
CDDP Target	×	✓	Learned	0.91 $\pm$ 0.04	3.56 $\pm$ 0.12
			Learned	<b>0.87 <math>\pm</math> 0.03</b>	<b>3.35 <math>\pm</math> 0.15</b>

maintaining an external memory with learned or unlearned content. Table 2 shows a map of model variants corresponding to the activation status of these three design choices, as well as the corresponding numerical results on the Sine Waves data set over five repetitions. We observe a performance increase when knowledge transfer is done via the external memory *instead of—but not together with*—parameter transfer, supporting the central assumptions of our target model. Setting the memory content to unlearned values causes rapid performance deterioration as values diverge from the learned values. This outcome demonstrates the essential role of the external memory in the continual learning performance of CDDP.

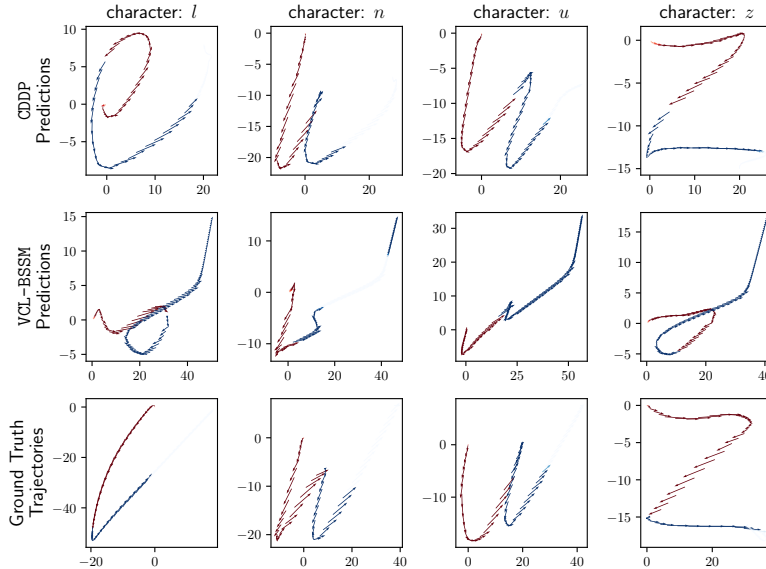


Figure 4: Predictions of CDDP (top row) and VCL-BSSM (middle row) on sample sequences from four tasks of the Character Trajectories data set after continual learning is over. Bottom row shows the corresponding ground-truth trajectories. The first one-third of each trajectory is considered as context (plotted in red), and the rest is predicted by the models (plotted in blue). Our CDDP remembers the first task much more precisely than VCL-BSSM (first and second columns) after adapting itself accurately to the last task (third and fourth columns). This is achieved by virtue of its external episodic memory.

## 7 Conclusion

**Summary.** We report the first study on continual learning of multi-modal dynamical systems. We curate a competitive baseline for this new problem setup from an adaptation of VCL to BSSMs. We introduce a novel alternative to the parameter transfer approach of VCL for within-task knowledge acquisition and cross-tasks knowledge transfer using an original combination of neural episodic memory, Dirichlet processes, and BSSMs. We observe in continual learning of challenging multi-modal dynamics modeling environments that our alternative approach compares favorably to the established parameter transfer approach.

**Broad Impact.** Our work can be used for numerous applications such as: i) weather forecasting, where features can be transferred from one climate to another, ii) autonomous driving, where driving patterns can be adapted across different countries, and iii) model-based reinforcement learning algorithms, when the environment changes due either to the actions of the ego agent or to external factors. The memory architecture of CDDP may be improved by alternative embedding, update, and attention mechanisms. Our formulation of the transition rule is agnostic to the architecture that governs the transition kernel. Transformer Networks [36], Neural Stochastic Differential Equations [17], or a blend of recent approaches can be used as a transition rule instead of the plain RNN.

**Limitations and Ethical Concerns.** CDDP demonstrates high sensitivity to the performance of its base model on individual tasks. The interpretability of the memory descriptors of the CDDP deserves further investigation. We present CDDP as a general-purpose method, hence its use in fairness-sensitive applications may require post-hoc allocation of existing fairness-inducing algorithms. The uncertainty calibration footprint of CDDP calls for another empirical study prior to its deployment into safety-critical setups.

## References

- [1] K.J. Åström. *Introduction to stochastic control theory*. Courier Corporation, 2012.

- [2] A. Chaudhry, M. Ranzato, M. Rohrbach, and M. Elhoseiny. Efficient lifelong learning with A-GEM. In *ICLR*, 2019.
- [3] K. Cho, B. van Merriënboer, D. Bahdanau, and Y. Bengio. On the properties of neural machine translation: Encoder-decoder approaches. *arXiv preprint arXiv:1409.1259*, 2014.
- [4] M.P. Deisenroth and C. Rasmussen. PILCO: A model-based and data-efficient approach to policy search. In *ICML*, 2011.
- [5] A. Doerr, C. Daniel, M. Schiegg, N. Duy, S. Schaal, M. Toussaint, and T. Sebastian. Probabilistic recurrent state-space models. In *ICML*, 2018.
- [6] D. Dua and C. Graff. UCI machine learning repository, 2017.
- [7] C. Finn, P. Abbeel, and S. Levine. Model-agnostic meta-learning for fast adaptation of deep networks. In *ICML*, 2017.
- [8] E.B. Fox, E.B. Sudderth, M.I. Jordan, and A.S. Willsky. A sticky HDP-HMM with application to speaker diarization. *The Annals of Applied Statistics*, pages 1020–1056, 2011.
- [9] M. Fraccaro, D.J. Rezende, Z. Zwols, A. Pritzel, S.M.A. Eslami, and F. Viola. Generative temporal models with spatial memory for partially observed environments. In *ICML*, 2018.
- [10] R. Frigola, Y. Chen, and C. E. Rasmussen. Variational Gaussian process state-space models. In *NeurIPS*, 2014.
- [11] M. Garnelo, J. Schwarz, D. Rosenbaum, F. Viola, D.J. Rezende, S.M. Eslami, and Y.W. Teh. Neural processes. *arXiv preprint arXiv:1807.01622*, 2018.
- [12] A. Graves, G. Wayne, and I. Danihelka. Neural Turing Machines. *arXiv preprint arXiv:1410.5401*, 2014.
- [13] G. Graves, G. Wayne, M. Reynolds, T. Harley, I. Danihelka, A. Grabska-Barwinska, S.G. Colmenarejo, E. Grefenstette, T. Ramalho, J. Agapiou, A.P. Badia, K.M. Hermann, Y. Zwols, G. Ostrovski, A. Cain, H. King, C. Summerfield, P. Blunsom, K. Kavukcuoglu, and D. Hassabis. Hybrid computing using a neural network with dynamic external memory. *Nature*, 538:471–476, 2016.
- [14] Y. Guo, M. Liu, T. Yang, and T. Rosing. Improved schemes for episodic memory-based lifelong learning. *NeurIPS*, 2020.
- [15] D. Hafner, T. Lillicrap, J. Ba, and M. Norouzi. Dream to control: Learning behaviors by latent imagination. In *ICLR*, 2020.
- [16] D. Hafner, T. Lillicrap, I. Fischer, R. Villegas, D. Ha, H. Lee, and J. Davidson. Learning latent dynamics for planning from pixels. In *ICML*, 2019.
- [17] M. Haußmann, S. Gerwinn, A. Look, B. Rakitsch, and M. Kandemir. Learning partially known stochastic dynamics with empirical PAC Bayes. In *AISTATS*, 2021.
- [18] S. Hochreiter and J. Schmidhuber. Long short-term memory. *Neural computation*, 9:1735–80, 12 1997.
- [19] A.D. Ialongo, M. van der Wilk, J. Hensman, and C.E. Rasmussen. Overcoming mean-field approximations in recurrent Gaussian process models. In *ICML*, 2019.
- [20] M. Kandemir, A. Akgül, M. Haussmann, and G. Unal. Evidential Turing processes. In *ICLR*, 2022.
- [21] H. Kim, A. Mnih, J. Schwarz, M. Garnelo, A. Eslami, D. Rosenbaum, O. Vinyals, and Y.W. Teh. Attentive neural processes. In *ICLR*, 2019.
- [22] D.P. Kingma and J. Ba. Adam: A method for stochastic optimization. *arXiv preprint arXiv:1412.6980*, 2014.

- [23] J. Kirkpatrick, R. Pascanu, N. Rabinowitz, J. Veness, G. Desjardins, A.A. Rusu, K. Milan, J. Quan, T. Ramalho, A. Grabska-Barwinska, D. Hassabis, C. Clopath, D. Kumaran, and R. Hadsell. Overcoming catastrophic forgetting in neural networks. *Proceedings of the National Academy of Sciences*, 114(13), 2017.
- [24] N. Loo, S. Swaroop, and R.E. Turner. Generalized variational continual learning. In *ICLR*, 2021.
- [25] D. Lopez-Paz and M. Ranzato. Gradient episodic memory for continual learning. In *NeurIPS*, 2017.
- [26] C.V. Nguyen, Y. Li, T.D. Bui, and R.E. Turner. Variational continual learning. In *ICLR*, 2018.
- [27] J. Pitman et al. Combinatorial stochastic processes. Technical report, 2002.
- [28] H. Ramsauer, B. Schäfl, J. Lehner, P. Seidl, M. Widrich, T. Adler, L. Gruber, M. Holzleitner, M. Pavlovic ´, G.K. Sandve, V. Greiff, D. Kreil, M. Kopp, G. Klambauer, J. Brandstetter, and S. Hochreiter. Hopfield networks is all you need. In *ICLR*, 2021.
- [29] A. Rios and L. Itti. Closed-loop memory GAN for continual learning. In *IJCAI*, 2019.
- [30] V.G. Satorras, Z. Akata, and M. Welling. Combining generative and discriminative models for hybrid inference. In *NeurIPS*, 2019.
- [31] J. Sethuraman. A constructive definition of Dirichlet priors. *Statistica Sinica*, 4(2):639–650, 1994.
- [32] G. Singh, J. Yoon, Y. Son, and S. Ahn. Sequential neural processes. In *NeurIPS*, 2019.
- [33] J. Snell, K. Swersky, and R.S. Zemel. Prototypical networks for few-shot learning. In *NeurIPS*, 2017.
- [34] X. Su, S. Guo, T. Tan, and F. Chen. Generative memory for lifelong learning. *IEEE Transactions on Neural Networks and Learning Systems*, 31(6):1884–1898, 2020.
- [35] Y.W. Teh, M.I. Jordan, M.J. Beal, and D.M. Blei. Hierarchical Dirichlet processes. *Journal of the American Statistical Association*, 101(476):1566–1581, 2006.
- [36] A. Vaswani, N. Shazeer, N. Parmar, J. Uszkoreit, L. Jones, A.N. Gomez, L. Kaiser, and I. Polosukhin. Attention is All you Need. In *NeurIPS*, 2017.
- [37] C. Yildiz, M. Heinonen, and H. Lähdesmäki. ODE<sup>2</sup>VAE: Deep generative second order ODEs with Bayesian neural networks. In *ICML*, 2019.
- [38] F. Zenke, B. Poole, and S. Ganguli. Continual learning through synaptic intelligence. In *ICML*, 2017.

## A Appendix

### A.1 Derivations

#### A.1.1 ELBO for basic BSSM

Applying Jensen’s inequality in the conventional way, the corresponding ELBO will be

$$\begin{aligned}
& \log p(y_{1:T}) \\
&= \log \int_{X,\theta} p(y_{1:T}|x_{1:T})p(x_{1:T}|\theta, x_0)p(x_0)p(\theta) \\
&= \log \int_{X,\theta} \left\{ \frac{p(y_{1:T}|x_{1:T})p(x_{1:T}|\theta, x_0)p(x_0)p(\theta)}{p(x_{1:T}|\theta, x_0)q_\xi(x_0|y_{1:C})q_\psi(\theta)} \times q_\xi(x_0|y_{1:C})p(x_{1:T}|\theta, x_0)q_\psi(\theta) \right\} \\
&\geq \mathbb{E}_{p(x_{1:T}|\theta, x_0)q_\xi(x_0|y_{1:C})q_\psi(\theta)} [\log p(y_{1:T}|x_{1:T})] - KL(q_\xi(x_0|y_{1:C})||p(x_0)) \\
&\quad - KL(q_\psi(\theta)||p(\theta)). \tag{17}
\end{aligned}$$

where  $KL(\cdot||\cdot)$  stands for the Kullback-Leibler (KL) divergence between the two distributions on its arguments, and  $X = \{x_0, \dots, x_T\}$ .

#### A.1.2 ELBO for Our Model CDDP

$$\begin{aligned}
& \log p(y_{1:T}) \\
&= \log \int_{X,\theta} \sum_{r=1}^R \pi_r p(y_{1:T}|x_{1:T})p(x_{1:T}|\theta, x_0, m_r)p(x_0)p(\theta) \\
&= \log \int_{X,\theta} \sum_{r=1}^R \pi_r \left\{ \frac{p(y_{1:T}|x_{1:T})p(x_{1:T}|\theta, x_0, m_r)p(x_0)p(\theta)}{p(x_{1:T}|\theta, x_0, m_r)q_\xi(x_0|y_{1:C})q_\xi(\pi = r|y_{1:C})q_\psi(\theta)} \right. \\
&\quad \left. \times p(x_{1:T}|\theta, x_0, m_r)q_\xi(x_0|y_{1:C})q_\xi(\pi = r|y_{1:C})q_\psi(\theta) \right\} \\
&\geq \mathbb{E}_{p(x_{1:T}|\theta, x_0, m_r)q_\xi(x_0|y_{1:C})q_\psi(\theta)q_\xi(\pi=r|y_{1:C})} [\log p(y_{1:T}|x_{1:T})] - KL(q_\xi(x_0|y_{1:C})||p(x_0)) \\
&\quad - KL(q_\psi(\theta)||p(\theta)) - \sum_{r=1}^R w_r(m_r, y_{1:C}) \log(w_r(m_r, y_{1:C})/\pi_r). \tag{18}
\end{aligned}$$

## A.2 Details on Synthetic Data Sets, Hyperparameters, and Architectures

Each experiment repetition presents the tasks to the continual learning models at random order.

### Data:

- i) Synthetic Data Sets: Each synthetic data set has 12 train sequences and 6 test sequences per mode. There are 15 modes 5 tasks in Sine Waves, 8 modes 4 tasks in Lotka-Volterra and 12 modes 4 tasks in Lorenz Attractor. We set the sequence lengths and time steps  $(T, \Delta t)$  to (15, 0.1) for Sine Waves, (25, 0.4) for Lotka-Volterra, and (50, 0.01) for the Lorenz Attractor. For each mode in the whole data set, we generate a long sequence and divide the whole sequence into subsequences of length  $T$  with a certain space between them. For all synthetic data sets, fixed jump space between subsequences is 5 time-point. By adding additional Gaussian noise to the train split, we construct train and test splits with these subsequences.

Sine Waves) We generate different modes from five different choices for  $A \in [3, 6, 9, 12, 15]$ , and three frequency levels for  $f \in [\frac{2}{3}, 1, \frac{4}{3}]$ . We add Gaussian noise from  $\mathcal{N}(0, \sigma)$  and set  $\sigma$  to  $\frac{A}{100}$  for each mode to the train split.

Lotka-Volterra We generate different modes by setting the free parameter pairs  $(\alpha, \delta)$  and  $(\beta, \gamma)$  to different values. Starting with a fixed point  $(x_0, y_0) = (2, 2)$ , we select levels as  $\alpha, \beta, \gamma \in [0.25, 0.75]$ , and a constant  $\delta = 0.5$ . We add a Gaussian noise from  $\mathcal{N}(0, 0.001)$  to the train split.

Lorenz Attractor We determine our modes by settings the free parameters  $\sigma, \rho$ , and  $\beta$  of the Lorenz system to different values. We start with initial state  $(x_0, y_0, z_0) = (1, 1, 28)$  and generate a long sequence. We generate modes with different but partially overlapping dynamical characteristics by setting  $\rho$  to three and  $\sigma$  and  $\beta$  to two different values. We select the three free parameters levels as  $\rho \in [28, 42, 56]$ ,  $\sigma \in [8, 12]$ , and  $\beta \in [\frac{5}{3}, \frac{13}{3}]$ . We add Gaussian noise from  $\mathcal{N}(0, 0.01)$  to the train split.

ii) Libras: The data set has 12 train sequences and 12 test sequences per mode. There are 15 modes 5 tasks. The sequence lengths and time step  $(T, \Delta t)$  are  $(45, \frac{7}{45})$ . There are no fixed  $\Delta$  for this data set but to find it we divide the approximate seconds taken for a sample to the number of frame count.

iii) Character Trajectories: The data set has different number of instances per modes therefore, we divide each instances samples to two halves then first half is placed in the train split and rest of them are placed in the test split. Hence, train split has 1422 samples, and test split with 1436 samples In the data set, each character is created with a different sequence length, to adapt the data set to our pipeline we subsample the sequences with the smallest sequence length which is 109. The sequence lengths and time step  $(T, \Delta t)$  are  $(109, 0.05)$ .

**Context Length Selection.** We select context length empirically as one-third of the sequence length amounting to five for Sine Waves, eight for Lotka-Volterra, 16 for the Lorenz Attractor, 15 for Libras, and 35 for Character Trajectories. The reason for that is, generally, one-third of the sequence captures the general characteristic of the dynamics and gives indications about modes.

**Architectures.** Our CDDP has four main architectural elements:

i) Encoder: The sequence encoder  $e_\lambda(x_{t:t'})$  governs the mean of our normal distributed recognition model  $q_\psi(x_0|y_{1:C}, \pi)$ . We feed  $C$  observations as a stacked set of values into the encoder. The sequence encoder is a single dense layer for Sine Waves, Lotka-Volterra, Libras; and a multi-layer perceptron for the Lorenz Attractor, and Character Trajectories with two hidden layers of size 90. The perceptron uses the  $\tanh(\cdot)$  activation function followed by layer normalization.

ii) Decoder: The likelihood function  $p(y_t|x_t)$  of the base model serves as a probabilistic decoder that maps the latent state  $x_t$  to the observed state  $y_t$ . We choose the emission distribution to be normal with mean governed by a single dense layer for Sine Waves, Lotka-Volterra, Libras; and a multilayer perceptron with two hidden layers of size 90 for the Lorenz Attractor, and Character Trajectories. The perceptron uses the  $\tanh(\cdot)$  activation function followed by layer normalization.

iii) Transition Kernel: We choose the transition kernel  $p(x_t|x_{t-1}, m, \theta)$  of CDDP to be a normal distribution with mean governed by a plain RNN that receives a concatenation of the previous hidden state and the mode descriptor as input. All covariates are set to a fixed variance of 0.1. The RNN on the mean is a multilayer perceptron with one hidden layer of size 40 for Sine Waves, Lotka-Volterra, and Libras; and 90 for the Lorenz Attractor, Character Trajectories. The perceptron uses the  $\tanh(\cdot)$  activation function followed by layer normalization. The transition kernel of the base model of VCL  $p(x_t|x_{t-1}, \theta)$  follows the same RNN architecture except that its input does not contain a mode descriptor.

iv) External Memory: We set the memory size to 20 for the Sine Wave environment, 10 for Lotka-Volterra, 15 for the Lorenz Attractor, 20 for Libras, and 30 for Character Trajectories.

### A.3 Detailed on Main Results

We provide a detailed results of the experiments in Table 3.

Table 3: Quantitative results of models on five data sets. The reported numbers are mean  $\pm$  standard error over 10 repetitions.

Data Set	Model	Score	1 Task	2 Tasks	3 Tasks	4 Tasks	5 Tasks
Sine Waves	VCL-BSSM	NMSE	<b>0.13 <math>\pm</math> 0.02</b>	0.97 $\pm$ 0.14	1.22 $\pm$ 0.15	1.27 $\pm$ 0.09	1.39 $\pm$ 0.08
		NLL	<b>1.76 <math>\pm</math> 0.22</b>	3.75 $\pm$ 0.24	3.84 $\pm$ 0.13	4.20 $\pm$ 0.15	4.29 $\pm$ 0.10
	CDDP	NMSE	0.16 $\pm$ 0.02	<b>0.88 <math>\pm</math> 0.11</b>	<b>1.07 <math>\pm</math> 0.15</b>	<b>1.12 <math>\pm</math> 0.14</b>	<b>1.31 <math>\pm</math> 0.11</b>
		NLL	2.09 $\pm$ 0.27	<b>3.43 <math>\pm</math> 0.22</b>	<b>3.77 <math>\pm</math> 0.17</b>	<b>4.05 <math>\pm</math> 0.14</b>	<b>4.15 <math>\pm</math> 0.10</b>
Lotka-Volterra	VCL-BSSM	NMSE	0.17 $\pm$ 0.03	<b>0.71 <math>\pm</math> 0.08</b>	<b>0.92 <math>\pm</math> 0.15</b>	<b>0.53 <math>\pm</math> 0.03</b>	
		NLL	0.56 $\pm$ 0.20	1.97 $\pm$ 0.28	<b>2.02 <math>\pm</math> 0.19</b>	<b>1.46 <math>\pm</math> 0.12</b>	
	CDDP	NMSE	<b>0.13 <math>\pm</math> 0.03</b>	0.72 $\pm$ 0.20	0.96 $\pm$ 0.18	0.60 $\pm$ 0.05	
		NLL	<b>0.32 <math>\pm</math> 0.18</b>	<b>1.35 <math>\pm</math> 0.21</b>	2.05 $\pm$ 0.15	1.54 $\pm$ 0.21	
Lorenz Attractor	VCL-BSSM	NMSE	0.22 $\pm$ 0.02	0.25 $\pm$ 0.03	0.27 $\pm$ 0.02	0.28 $\pm$ 0.01	
		NLL	4.22 $\pm$ 0.16	4.41 $\pm$ 0.08	4.55 $\pm$ 0.09	4.52 $\pm$ 0.04	
	CDDP	NMSE	<b>0.21 <math>\pm</math> 0.02</b>	<b>0.24 <math>\pm</math> 0.02</b>	<b>0.25 <math>\pm</math> 0.02</b>	<b>0.26 <math>\pm</math> 0.02</b>	
		NLL	<b>4.06 <math>\pm</math> 0.19</b>	<b>4.33 <math>\pm</math> 0.02</b>	<b>4.53 <math>\pm</math> 0.06</b>	<b>4.46 <math>\pm</math> 0.03</b>	
Libras	VCL-BSSM	NMSE	<b>0.13 <math>\pm</math> 0.01</b>	0.14 $\pm$ 0.00	<b>0.13 <math>\pm</math> 0.01</b>	0.15 $\pm$ 0.00	<b>0.14 <math>\pm</math> 0.00</b>
		NLL	-0.41 $\pm$ 0.04	-0.35 $\pm$ 0.03	<b>-0.42 <math>\pm</math> 0.04</b>	-0.32 $\pm$ 0.03	-0.36 $\pm$ 0.03
	CDDP	NMSE	0.14 $\pm$ 0.00	<b>0.13 <math>\pm</math> 0.01</b>	0.14 $\pm$ 0.01	<b>0.14 <math>\pm</math> 0.01</b>	<b>0.14 <math>\pm</math> 0.01</b>
		NLL	<b>-0.42 <math>\pm</math> 0.03</b>	<b>-0.40 <math>\pm</math> 0.04</b>	-0.38 $\pm$ 0.05	<b>-0.40 <math>\pm</math> 0.03</b>	<b>-0.37 <math>\pm</math> 0.04</b>
Character Trajectories	VCL-BSSM	NMSE	<b>0.42 <math>\pm</math> 0.04</b>	0.80 $\pm$ 0.04	0.90 $\pm$ 0.02	1.11 $\pm$ 0.08	1.11 $\pm$ 0.10
		NLL	<b>-0.23 <math>\pm</math> 0.06</b>	0.06 $\pm$ 0.05	0.20 $\pm$ 0.05	0.31 $\pm$ 0.08	0.35 $\pm$ 0.09
	CDDP	NMSE	0.52 $\pm$ 0.05	<b>0.56 <math>\pm</math> 0.02</b>	<b>0.69 <math>\pm</math> 0.04</b>	<b>0.71 <math>\pm</math> 0.03</b>	<b>0.71 <math>\pm</math> 0.02</b>
		NLL	-0.05 $\pm$ 0.05	<b>-0.26 <math>\pm</math> 0.04</b>	<b>-0.17 <math>\pm</math> 0.03</b>	<b>-0.23 <math>\pm</math> 0.04</b>	<b>-0.26 <math>\pm</math> 0.04</b>

#### A.4 Details on Experimental Procedure

We select Adam [22] as optimizer with learning rates of 0.005 for Sine Waves, 0.001 for Lotka-Volterra, 0.0005 for Lorenz Attractor, 0.001 for Libras, and 0.001 for Character Trajectories. For all data sets, the batch size is equal to 9 except for Character Trajectories which is equal to 64 due to high number of instances. We train the models 300 for Sine Waves, 750 for Lotka-Volterra, 500 for Lorenz Attractor, 300 for Libras, and 2000 for Character Trajectories epochs per task.

We performed our experiments on Intel Xeon CPU E5-2650 v3 with 10 cores and Intel Core(TM) i7-6700K CPU with 4 cores.